Theor. Exp. Plant Physiol. (2022) 34:381–393
https://doi.org/10.1007/s40626-022-00251-3

The effects of *SBEIIb* gene mutation on physicochemical properties of starch in maize

Nan Han · Wanchen Li · Chuanxiao Xie · Fengling Fu

Received: 20 February 2022 / Accepted: 26 May 2022 / Published online: 21 July 2022

Abstract Maize (*Zea mays* L.) is one of the most important crops in the world. In the starch industry and nutraceutical fields, maize (*Zea mays* L.) varieties containing a high percentage of amylose show considerable value because of the ability to form gels and films, and to be used as a source for production of resistant starch, which may prevent diseases such as diabetes and obesity. The *SBEIIb* gene encodes the starch-branching enzyme, SBEIIb, one of the starch-branching isozymes (SBEI, SBEIIa, and SBEIIb). The *amylose-extender* (*ae/sbe2b*) locus is the structural gene for SBEIIb. Its recessive mutant *ae/sbe2b* decreases the total activities of the SBEs and increases the amylose proportion from 20 to 30% up to 70%. To evaluate the effects of *SBEIIb* gene mutation on the starch concentration, physicochemical properties of endosperm starch and agronomic traits, we genotyped the high-amylose germplasm line GEMS-0067 for the *ae/sbe2b* mutation. We also measured starch concentration, amylose proportion and major agronomic traits, and observed the morphology of starch granules through scanning electron microscopy (SEM). We additionally determined the physicochemical properties of high-amylose endosperm starch, including gelatinization properties, thermal properties and the degree of starch chain polymerization by using rapid viscosity analysis (RVA), differential scanning calorimetry (DSC) and high-performance anion-exchange chromatography (HPAEC). The production of high-amylose starch, the typical irregular starch granules and the typical physicochemical properties of high amylose endosperm starch suggested the deletion of the ninth exon of *SBEIIb* increased the amylose concentration and further affected the physicochemical properties of maize starch. Its useful gelatinization and thermal properties, and the degree of polymerization of the starch chains demonstrated the advantages of using GEMS-0067 as a commercial variety with high-amylose starch for applications in the starch industry and nutraceutical fields, and as a parental strain for high-amylose maize breeding.

N. Han · W. Li · F. Fu (✉)
Key Laboratory of Biology and Genetic Improvement of Maize in Southwest Region, Ministry of Agriculture, Maize Research Institute, Sichuan Agricultural University, Chengdu 611130, China
e-mail: ffl@sicau.edu.cn

N. Han
e-mail: han_nan199068@163.com

W. Li
e-mail: aumdyms@sicau.edu.cn

C. Xie (✉)
Institute of Crop Sciences, Chinese Academy of Agricultural Sciences, Beijing 100081, China
e-mail: xiechuanxiao@caas.cn

C. Xie
National Key Facility for Crop Gene Resources and Genetic Improvement, Beijing 100081, China

Keywords *Ae* mutant · Amylose · Breeding potential · Maize · SBEIIb · Physicochemical properties

1 Introduction

Maize (*Zea mays* L.) is a major staple food crop worldwide (Andorf et al. 2019). The kernels contain large amounts of starch, consisting of essentially linear amylose and highly branched amylopectin (Myers et al. 2000). The concentration and proportion of amylose and amylopectin determine the quality and usage of the maize (Glaring et al. 2006). Native starch granules in cereal endosperm usually comprise 20–30% amylose and 70–80% amylopectin (Goren et al. 2018). In waxy maize, which is grown as a food crop, especially in East and Southeast Asia, the proportion of amylopectin can be as high as almost 100% (Liu et al. 2007; He et al. 2020), whereas high-amylose varieties, with amylose proportions of more than 50%, are not only particularly valuable for the starch industry but are also used to control dietary carbohydrate intake (Cai et al. 2014; Lin et al. 2016; Wang et al. 2017). These two advantages have led to increased interest in the use of high amylose starches. High-amylose starch is widely used in numerous industrial applications, such as starch-based gels, films, textiles, gum candies and cosmetics (Zhang et al. 2020). It also has great potential for use in the food and nutraceutical fields because of its high levels of resistant starch (RS), which is refractory to gelatinization and hydrolysis, and cannot be readily digested in the upper gastrointestinal tract (Koch et al. 2010; Raigond et al. 2015; Lin et al. 2016; Zhang et al. 2016; Song et al. 2019). Resistant starch has been reported to provide many health benefits in humans, including decreasing the risk of developing diabetes and obesity (Cai et al. 2014). Therefore, maize improvement to achieve higher percentages of amylose has attracted considerable attention in recent years (Bear et al. 1958; Jeon et al. 2010; Jiang et al. 2013).

The proportion of amylose in maize endosperm starch is controlled by a series of starch synthesis genes (Liu et al. 2007; Goren et al. 2018; Li et al. 2018; Song et al. 2019; He et al. 2020). One of the most critical genes is the *SBEIIb* gene that encodes the starch-branching enzyme SBEIIb (one of the SBE isozymes: SBEI, SBEIIa, and SBEIIb). The full-length sequence of SBEIIb is 23,449 bp long and it contains 22 exons (Bear et al. 1958; Guan and Preiss 1993; Liu et al. 2007; Goren et al. 2018; Li et al. 2018; Song et al. 2019; He et al. 2020; Zhong et al. 2020). The *amylose-extender* (*ae/sbe2b*) locus is the structural gene for SBEIIb and the amylose proportion in its recessive mutant *ae* is greater than 60% (Kim et al. 1998; Fuwa et al. 1999; Li et al. 2008; Jiang et al. 2010; Liu et al. 2015). For example, the total activities of SBEs in an *ae* mutant decreased to about 71% of those in its wild-type (WT) control because of the deletion of the ninth exon of the *SBEIIb* gene, containing 84 bases (Kim et al. 1998; Fuwa et al. 1999; Li et al. 2008; Jiang et al. 2010; Liu et al. 2015). When *SBEIIb* is mutated, the enzyme complex, consisting of starch synthesis enzymes, may become looser or may even not form (Liu et al. 2007; Lin et al. 2016; Wang et al. 2017), leading to a decrease in amylopectin percentage and a consequent increase in amylose percentage. Thus, the amylose proportion of this line was as high as 70% (Liu et al. 2007; Lin et al. 2016; Wang et al. 2017; He et al. 2020). Furthermore, the inactivation of SBE activity and the increased amylose concentration may induce important effects on the physicochemical properties of starch. The inhibition of SBE expression tends to alter starch morphology and structure, thereby resulting in heteromorphous starch granules. For example, the starches from the *ae* mutant consist of approximately 7% elongated granules (Jiang et al. 2010). Likewise, starch with high-amylose concentration has been demonstrated to show enhanced resistance to gelatinization and hydrolysis (Wei et al. 2011).

Overall, we hypothesized that *SBEIIb* plays an important role in increasing amylose concentrations and altering physicochemical properties of starch. To test this hypothesis, we genotyped the high-amylose germplasm line GEMS-0067, released as a parent for high-amylose maize breeding by Truman State University (Campbell et al. 2007), and its wild-type (WT) control for the *ae/sbe2b* mutation, and performed phenotypic analysis of major agronomic traits. We additionally assessed the starch granule morphology, starch concentration and amylose proportion, gelatinization and thermal properties, and degree of starch chain polymerization through physiological and biochemical techniques, including scanning electron microscopy (SEM), light microscopy, rapid

viscosity analysis (RVA), differential scanning calorimetry (DSC) and high-performance anion-exchange chromatography (HPAEC). We provide information about the effects of mutations in key genes involved in starch synthesis, starch concentration and physicochemical properties of maize. Moreover, the results improve the understanding of *SBEIIb* and the physicochemical properties of high-amylose starch. Our findings may be useful for applications of high-amylose starches in industrial and maize breeding settings.

2 Material and methods

2.1 Plant material

The high-amylose GEMS-0067 line (*ae* mutant) and its WT control were used in this study. GEMS-0067 (Reg. no. GP-550, PI 643,420) is a partially inbred germplasm line and is currently maintained by sib-mating within the F5-derived line from the pedigree GUAT209:S13 × (H99*ae* × OH43*ae*). GEMS-0067 was released by Truman State University (Kirksville, MO, USA) for use in the development of genetically diverse, elite, Amylomaize Class VII (starch amylose > 70%) parental lines. GUAT209:S13 is a 50% tropical, exotic breeding cross, which was derived from crossing Guatemala 209 (PI 498583) to an inbred from a private cooperator designated as company 13. Only lines from GUAT209:S13 × (H99*ae* × OH43*ae*) were found to survive inbreeding and therefore used in subsequent breeding studies. Kernels of the original GUAT209:S13 × (H99*ae* × OH43*ae*) F_1 seed was planted. Resulting plants were self-pollinated and ears with segregating F_2 kernels (3 normal-type:1 *ae*-type). The WT was from segregating F_2 kernels (*Ae/Ae* homozygous genotype from normal-type) and GEMS-0067 was from segregating F_2 kernels (*ae/ae* homozygous genotype from *ae*-type) (Campbell et al. 2007).

2.2 Genotyping of the *ae/sbe2b* mutation

Genomic DNA was extracted separately from leaf samples of the germplasm line GEMS-0067 and the WT, using CTAB buffer (Maroof et al. 1985). The quality and quantity of DNA samples were determined on a NanoPhotometer™P-Class (Implen, Schatzbogen, Germany) and visualized by electrophoresis on 1% (w/v) agarose gel. The reference sequence of the WT *SBEIIb* gene (GenBank: AF072725.1) was downloaded from the NCBI database (https://www.ncbi.nlm.nih.gov/gene/?term=AF072725.1). Referring to the method of Kim et al. (1998), the genomic sequence from the 8th to 10th exon of the *SBEIIb* gene was amplified with a pair of specific primers (5′-CCAGCCTGGATCAAGTACTC-3′/5′-CTTGGATACAATGCAGTGCAA-3′), with the products separated by 1.5% agarose gel electrophoresis, subcloned into *pMD-19-T* vector, and sequenced at Sengon Biotech (Chengdu, China). The possible mutation of the *ae/sbe2b* gene was genotyped by alignment of the sequences between the line GEMS-0067 and the corresponding WT by using the SnapGene software (GSL Biotech LLC, San Diego, CA, USA).

2.3 Scanning electron microscopy

As described by Lin et al. (2016) and He et al. (2020), starch was isolated from mature endosperm, dried completely at 40 °C, mounted on an aluminum specimen holder using double-sided adhesive tape, sputter-coated with gold in a vacuum evaporator, and viewed under a scanning electron microscope (TM4000 Plus, Hitachi, Tokyo, Japan). The images of starch granules were obtained at an accelerating voltage of 10 kV and a magnification of ×4000.

2.4 Determination of starch concentration and percentage amylose

According to Yang et al. (2013), three replicates of kernel samples of each line (100 kernels per replicate of each line) were wetted with a calcium chloride: acetic acid solution (500 g calcium chloride were dissolved in 600 mL distilled water, with the pH value adjusted to 2.3 with acetic acid), hydrolyzed in a glycerin bath for 30 min at 119 ± 1 °C. After precipitating the protein by addition of zinc sulfate and potassium ferrocyanide solutions (30 g 100 mL^{-1} [w/v] zinc sulfate, 15 g 100 mL^{-1} [w/v] potassium ferrocyanide), the samples were adjusted to 100 mL volume with distilled water, filtered, and the rotation angle of the filtrate read in a polarimeter (MCP150, Anton Paar, Shanghai, China). Starch concentration was determined as:

$$\text{starch concentration (g/100g)} = \frac{\alpha \times 10^6}{L \times W\,(100 - H) \times 203}$$

where α, L, W, H, and 203 stand for the rotation angle, length (dm) of the polarizing tube, mass of sample, moisture concentration of sample, and specific rotation of starch, respectively.

The percentage amylose of the three replicates of each maize line was determined by using an amylose/amylopectin assay kit (Megazyme, Bray, Ireland), according to the manufacturer's instructions. After eliminating the possible lipids, proteins, and amylopectin by using ethanol and concanavalin A, the remaining amylose was enzymatically hydrolyzed to D-glucose, oxidized with glucose oxidase/peroxidase (GOPOD) reagent (Gibson et al. 1997), and the absorbance at 510 nm read in a spectrophotometer (UV5Nano, Mettler Toledo, Zurich, Switzerland).

2.5 Determination of starch physicochemical properties

As described by Wang et al. (2018a), the starch samples were homogenized and passed through a 200-mesh sieve, moisture concentration was determined in a rapid moisture meter (HR83-P, Mettler Toledo, Zurich, Switzerland), a 5-g (error < 0.05 g) sample was weighed out, transferred onto aluminum foil, mixed well with 25 mL sterile water, and the viscosity determined in a rapid viscosity analyzer (RVA Super 4, Newport Scientific, Jessup, MD, USA).

As described by Wang et al. (2018a), a 10-mg homogenized and sieved starch sample was added to 30 µl sterile water, incubated at room temperature for 24 h, heated from 30 to 95 °C at a heating rate of 10 °C/min and the transition temperatures (T_o, T_p, and T_c) were determined in a differential scanning calorimeter (DSC) (TA Instruments, New Castle, DE, USA). The gelatinization enthalpy (ΔH) was calculated using the software of the instrument.

As described by Hanashiro et al. (1996), the starch samples were dissolved in 50 mM sodium acetate and debranched with isoamylase (Sigma, Darmstadt, Germany). The degree of polymerization (chain length distribution) was determined and analyzed by high-performance anion-exchange chromatography (HPAEC) (Thermo Fisher Scientific, Waltham, MA, USA) via pulsed amperometric detection. A Dionex™ CarboPac™ PA10 (250×4.0 mm I.D., 10 µm particle size) liquid chromatographic column was used, with an injection volume of 20 µl and a mobile phase A (200 mM NaOH) and mobile phase B (200 mM NaOH/200 mM NaAc). The isocratic elution conditions of the mobile phase are as follows: 0–14.0 min 90% phase A/10% B, 14.1–17.0 min 40% A/60% B, 17.1–22.0 min 90% A/10% B, the column temperature was 30 °C, the flow rate was 0.3 mL min^{-1} and the monosaccharide components were analyzed and detected by an electrochemical detector.

2.6 Phenotyping of agronomic traits

The field experiments comparing the two lines were conducted in the summer and autumn of May and November 2018–2019, respectively, and in the summer of May 2020. The field experiments were planted at Shunyi, Beijing, China Experimental Station (40° 23×74.3″ N, 116° 57×03.5″ E) in the summer and were planted at Huangliu, Hainan, China Experimental Station (18° 52×65.1″ N, 108° 83×81.8″ E) in the autumn. Both stations are affiliated to the Chinese Academy of Agricultural Sciences.

The GEMS-0067 and the WT were transplanted to the field in a randomized complete block design with three replicates. Both lines were isolated from genetically modified and other maize materials to avoid cross-pollination and material mixing. Seedlings of uniform size and development status were selected for transplanting to ensure the survival rate and decrease environmental variation invariables. Each line was cultivated in three rows (630 cm long and 30 cm apart) per plot. Twenty-one plants were retained in each row. The study field is a sandy soil. The N-P-K compound fertilizer (at an N:P:K ratio of 15:15:15) as a base fertilizer was applied once at 50 kg per 0.067 hectare before sowing; additional fertilizer consisting of 20 kg urea per 0.067 hectare was applied in fertilization management. Manual and chemical methods were used for weed control, and conventional local management protocols, including irrigation, for maize cultivation, were followed. Growth status and disease resistance were observed over the entire growth period. To avoid edge-row effects, only the plants in the middle row of each plot were measured with respect to anthesis stage, silking stage, growth period, plant height, and ear height. At maturity stage, the flowers were bagged to avoid any cross pollination

before self-pollination, and the ears were harvested from the fifteen middle plants in the middle row of each plot, air dried, photographed, and row number per ear, kernel number per row, 100-kernel mass, and kernel mass per plant were determined for each replicate of each line. Subsequently, sample kernels were cut transversely and longitudinally, stained with I_2/KI solution (0.2 g I_2 and 2 g KI dissolved in 100 mL of distilled water) for 5 min as described by Hunt et al. (2013), and photographed under an optical microscope (Mshot, Guangzhou, China) at ×2 magnification.

2.7 Data analysis

The data were analyzed by Microsoft Excel 2013 (https://www.microsoft.com/) and Origin 8.0 software (https://www.originlab.com/) and presented as mean ± standard deviation (SD). The significance of the difference between the two lines was tested using Student's *t*-test, using SPSS software 11.2 (IBM, Armonk, NY, USA), as each of the variables approximated to a normal distribution, as analyzed by the Shapiro-Wilk ($n \leq 2000$) and Kolmogorov-Smirnov ($n > 2000$) tests, using SPSS software 11.2. The non-significance of these two tests indicated that the data satisfied the normal distribution for each variable, with a *p*-value of > 0.05.

3 Results

3.1 The *ae/sbe2b* gene

Genotype-specific 750-bp (GEMS-0067) and 1576-bp (WT) bands were separated from the amplified products of GEMS-0067 and its WT control, respectively (Fig. 1a). The full-length genomic sequence of the *SBEIIb* gene was 23,449 bp in the WT, and the structural organization of the gene in the two genotypes is shown in Fig. 1b. The results of sequencing and alignment studies showed that the entire 84 bases of the ninth exon in *SBEIIb* were deleted in GEMS-0067, as were 742 bases flanking regions (101-bp deletion in the intron between exons 8 and 9 and a 641-bp deletion in the intron between exons 9 and 10) (Fig. 1c).

3.2 Morphology of starch granules and amylose proportion

We observed the morphology of starch granules in mature maize endosperm and determined the starch concentrations and amylose proportions of the two genotypes. The scanning electron microscopy (SEM) images showed that the starch granules isolated from WT endosperm were spherical or elliptical, were large and had smooth surfaces, whereas the starch granules of GEMS-0067 contained individual or aggregated, elongated granules with irregular depressions, as well as an increased frequency of small subgranules, and were smaller than the normal individual granules (Fig. 2). The starch concentration and amylose proportion of GEMS-0067 on a dry mass basis were 72.63 (g 100^{-1} g) and 72.95%, respectively, both of which were significantly different from the 74.21 (g 100^{-1} g) and 26.26% values of WT, respectively (Table 1).

3.3 Gelatinization properties

Rapid viscosity analysis (RVA) is a useful tool to measure the pasting properties of maize starch. The results of RVA presented obvious differences in the viscosity curves between GEMS-0067 and WT starch (Fig. 3). In response to increasing temperature, the viscosity of WT starch gradually increased as a result of gelatinization, and presented a typical double-peak curve, whereas GEMS-0067 starch exhibited almost a horizontal straight line with only a small peak at the beginning (Fig. 3). The parameters of peak viscosity, through viscosity, break viscosity, final viscosity, and setback viscosity of GEMS-0067 starch were significantly lower than those of WT starch, whereas the peak time and gelatinization temperature values of GEMS-0067 starch were significantly higher than those of WT starch (Table 2).

3.4 Thermal properties

Differential scanning calorimetry indicated that the phase transition temperatures, including onset temperature (T_o), peak temperature (T_p) and conclusion temperature (T_c), of GEMS-0067 starch were significantly higher than those of WT starch, and that the gelatinization enthalpy of GEMS-0067 starch was significantly lower than that of WT starch (Table 3).

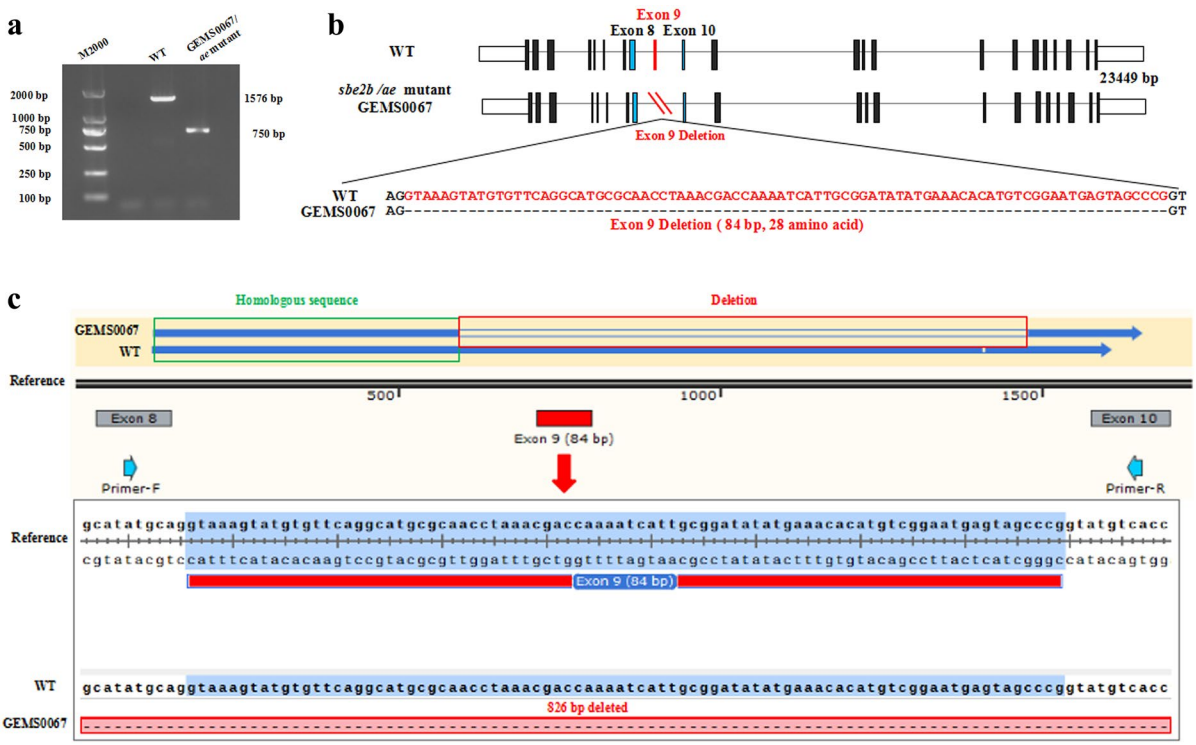

Fig. 1 The *ae/sbe2b* gene in GEMS-0067. **a** Specific bands separated from the amplified products of GEMS-0067 (750-bp) and WT (1576-bp). **b** The structural organization of the genomic sequences of the *ae/SBEIIb* gene in GEMS-0067 and WT. **c** The results of sequencing and alignment of the *ae/SBEIIb* gene between GEMS-0067 and WT by SnapGene software. The homologous sequences, deleted sequences, and the alignment results are marked by green, red, and gray boxes, respectively. The reference sequence of the WT *SBEIIb* gene (GenBank: AF072725.1) was downloaded from the NCBI database (https://www.ncbi.nlm.nih.gov/gene/?term=AF072725.1). The entire 84-bp sequence of the ninth exon in *SBEIIb* was deleted in GEMS-0067, together with the 742-bp flanking regions (101-bp deletion in the intron between exons 8 and 9 and a 641-bp deletion in the intron between exons 9 and 10)

In response to increasing temperature, the differential scanning calorimetry thermogram of WT starch presented an obvious absorption peak at 70 °C, whereas the absorption peak of the GEMS-0067 starch thermogram was almost a straight line (Fig. 4) because its gelatinization enthalpy was one-sixth that of WT (Table 3).

3.5 Degree of polymerization

The distribution of chain fractions in debranched amylopectin was determined by HPAEC. The result of HPAEC showed that the degree of polymerization (DP) depended heavily on the proportion of amylose and amylopectin in the starch. The percentage of short chains ($6 \le DP \le 24$) was lower in GEMS-0067 starch than in WT starch, whereas the percentages of medium chains ($25 \le DP \le 36$) and long chains ($DP \ge 37$) were higher in GEMS-0067 starch than in WT starch (Fig. 5).

3.6 Agronomic traits

Major agronomic traits were investigated to evaluate whether the agronomic performance changed with the *SBEIIb* gene mutation. Over the growth period, the two lines grew normally and were not infected by any pathogen. Analysis using Student's *t*-test showed that there were no significant differences between GEMS-0067 and WT in terms of the dates of anthesis or silking, duration of growth period, plant height, ear height, and row number per ear, thus indicating that the developmental traits and phenology were similar between GEMS-0067

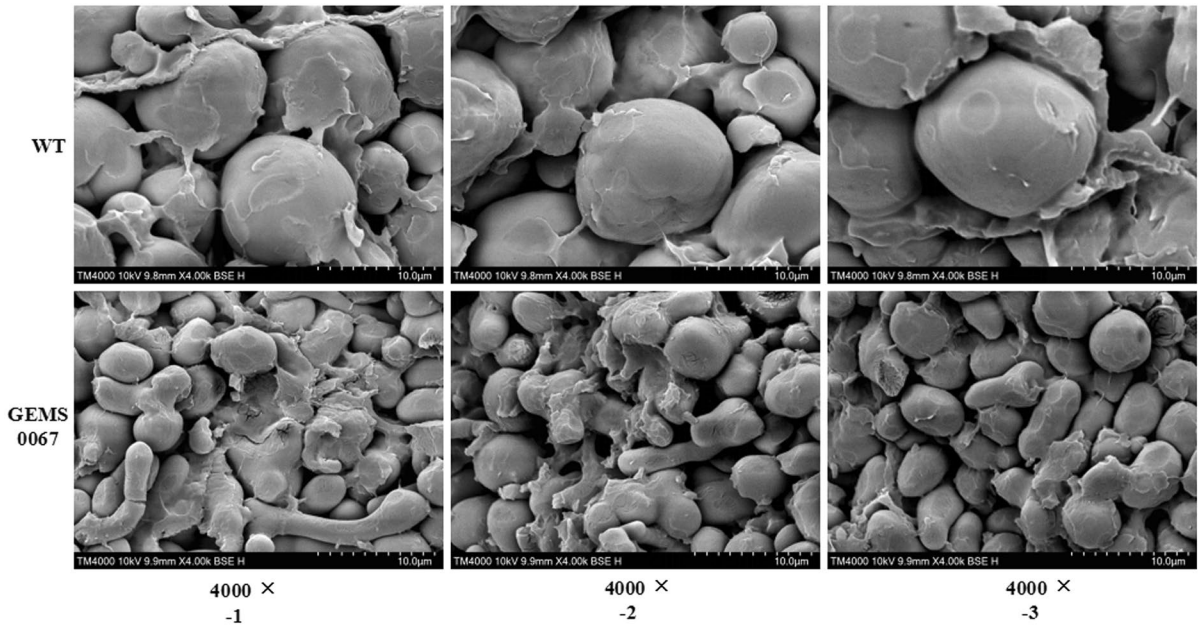

Fig. 2 SEM images of starch granules of GEMS-0067 and WT. The starch granules of WT were spherical or elliptical with smooth surfaces. The starch granules of GEMS-0067 were elongated with irregular depressions, as well as an increased frequency of small sub-granules. Scale bars: 10 µm, magnification: ×4000, and accelerating voltage: 10 kV. 4000× -1, 4000× -2 and 4000× -3 represent three different fields of view at ×4000 magnification

Table 1 Starch concentration and amylose proportion in the starch of GEMS-0067 and WT

	GEMS-0067	WT
Starch concentration (g 100^{-1} g)	72.63 ± 1.60[a]*	74.21 ± 2.08
Amylose proportion (%)	72.95 ± 1.39**	26.26 ± 1.60

[a]Values are presented as mean ± standard deviation of three biological replicates

* and ** indicate significant differences within the row between the two genotypes at $p < 0.05$ and $p < 0.01$ by Student's *t*-test, respectively

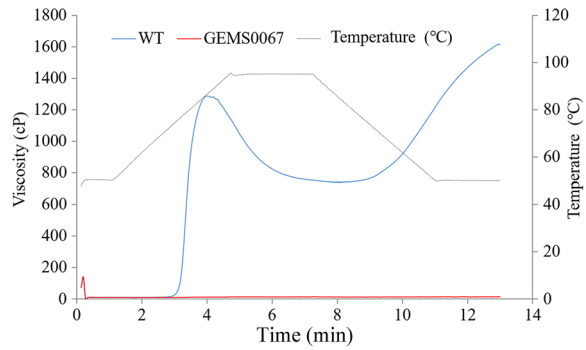

Fig. 3 Viscosity curves of GEMS-0067 and WT starch. The WT starch presented a typical double-peak curve, whereas GEMS-0067 starch demonstrated almost a horizontal straight line with a small peak at the beginning

and WT (Table 4). On the other hand, the GEMS-0067 kernels were slightly shrunken and duller, and had high amylose concentrations: the endosperm stained much darker and appeared predominantly blue after treatment with I_2/KI solution for 5 min, whereas the WT kernels were predominantly red (Fig. 6). GEMS-0067 showed a significantly lower 100-kernel mass and total kernel mass per ear, compared with WT, although its kernel number per row was significantly greater than that of WT (Table 4).

The single grain mass of GEMS-0067 was 0.25 g, a value 20% less than that of WT (0.3 g); similarly, the 100-kernel mass of GEMS-0067 was 85% that of the WT, whereas the kernel number per row of GEMS-0067 (28.06) was 1.98 more than that of the WT (26.08) on average.

Table 2 Gelatinization properties of starch of GEMS-0067 and WT

Property	GEMS-0067	WT
Peak viscosity (cP)	13.67 ± 1.15[a]**	1256.67 ± 32.02
Through viscosity (cP)	11.67 ± 1.15**	722.33 ± 23.46
Breakdown viscosity (cP)	2.00 ± 0.00**	534.33 ± 10.97
Final viscosity (cP)	13.00 ± 1.73**	1575.33 ± 37.69
Setback viscosity (cP)	1.33 ± 0.58**	853.00 ± 37.24
Peak time (min)	4.56 ± 0.41**	4.02 ± 0.04
Gelatinization temperature (°C)	> 95	75.18 ± 0.03

[a]Values are presented as mean ± standard deviation of three biological replicates. cP, centipoise

**Indicates significant differences within the row between the two genotypes for the same parameter at $p < 0.01$ by Student's *t*-test

Table 3 Thermal properties of starch of GEMS-0067 and WT

Property	GEMS-0067	WT
Onset temperature (°C)	73.38 ± 0.93[a]**	65.19 ± 0.15
Peak temperature (°C)	91.65 ± 2.97**	70.09 ± 0.03
Conclusion temperature (°C)	101.05 ± 0.09**	76.21 ± 0.13
Gelatinization enthalpy (J g^{-1})	2.33 ± 0.54**	12.60 ± 0.31

[a]Values are presented as mean ± standard deviation of three biological replicates

**Indicates significant differences within the row between the two genotypes for the same parameter at $p < 0.01$ by Student's *t*-test

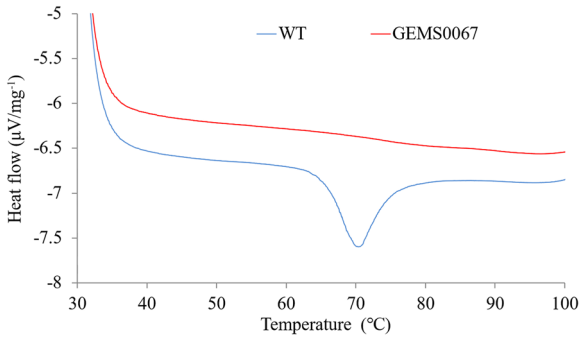

Fig. 4 Differential scanning calorimetry thermogram of GEMS-0067 and WT starch. The thermogram of WT starch presented an obvious absorption peak at 70 °C, whereas the GEMS-0067 starch thermogram was almost a straight line in response to increasing temperature. This result indicates that the starch of GEMS-0067 was more thermally stable than the WT starch

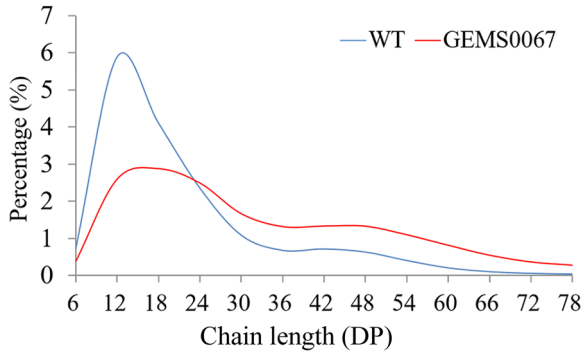

Fig. 5 Chain length (degree of polymerization, DP) of GEMS-0067 and WT starch. The percentage of short chains ($6 \le DP \le 24$) was lower, whereas the percentages of medium chains ($25 \le DP \le 36$) and long chains ($DP \ge 37$) were higher in GEMS-0067 starch than in WT starch

Table 4 Comparison of agronomic traits of GEMS-0067 and WT

Trait	GEMS-0067	WT
Anthesis stage (d)	56.06 ± 0.63[a]	55.00 ± 0.51
Silking stage (d)	60.08 ± 0.33	59.18 ± 0.44
Growth period (d)	101.38 ± 1.21	100.00 ± 1.24
Plant height (cm)	154.33 ± 5.40	152.65 ± 8.71
Ear height (cm)	70.11 ± 8.62	70.76 ± 5.64
Row number per ear	15.08 ± 0.63	14.91 ± 0.91
Kernel number per row	28.06 ± 1.20*	26.08 ± 1.51
Single grain mass (g)	0.25 ± 0.01*	0.30 ± 0.02
100-kernel mass (g)	25.63 ± 0.13*	30.33 ± 0.21
Kernel mass per ear (g)	107.51 ± 0.63**	117.34 ± 1.00

[a]Values are presented as mean ± standard deviation of three biological replicates

* and ** indicate significant differences within the row between the two genotypes for the same parameter at $p < 0.05$ and $p < 0.01$ by Student's *t*-test, respectively

4 Discussion

The *SBEIIb* gene is an endosperm-expressed gene that encodes one of the starch-branching enzyme (SBE) isozymes (SBEIIb) which play a critical role in the synthesis of amylopectin (Bear et al. 1958; Guan and Preiss 1993; Kim et al. 1998; Fuwa et al. 1999; Liu et al. 2007; Li et al. 2008, 2018; Goren et al. 2018; Song et al. 2019; He et al. 2020; Zhong et al. 2020). The enzyme complex, which is composed of starch synthesis enzymes, may become loose or even

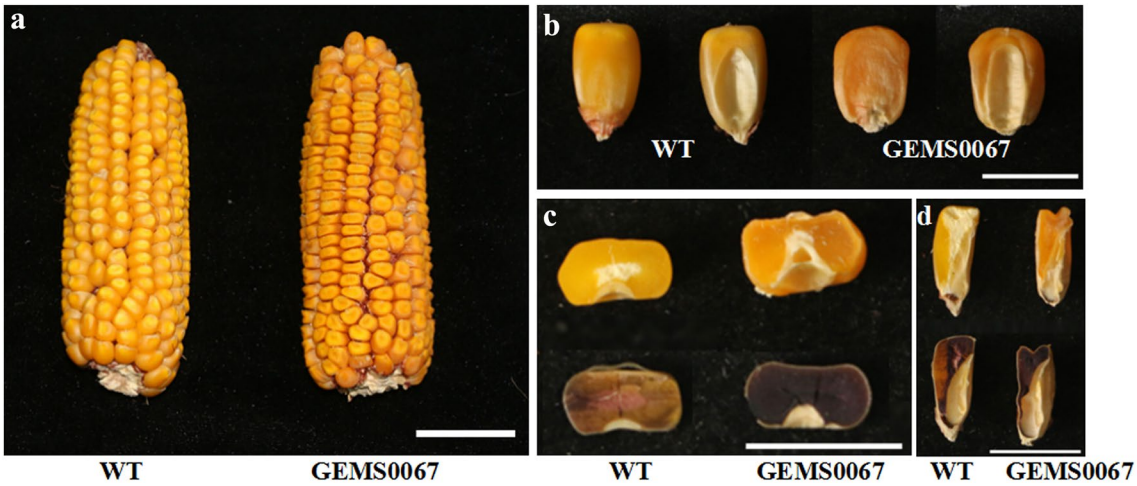

Fig. 6 Shrunken kernels and darker-stained endosperm of GEMS-0067. The kernel color of GEMS-0067 in Fig. 6a (external) and 6c (internal) was darker than that of the WT. The red color in sectioned WT kernels in Fig. 6c reflects the high amylopectin concentration of the WT starch whereas the blue color in sectioned GEMS-0067 kernels reflects the high amylose concentration in this line. **a** and **b** The kernels of GEMS-0067 were a little more shrunken and duller than WT. **c** and **d** A single maize kernel was sectioned and stained with I_2/KI solution for 5 min (0.2 g I_2 and 2 g KI dissolved in 100 mL of distilled water, diluted 100-fold with sterile water before use). The endosperm of GEMS-0067 was stained much darker and predominantly blue than that of WT (predominantly red). Scale bars: 3 cm (**a**) and 1 cm (**b**, **c**, **d**)

may not form with the mutation of the *SBEIIb* gene (Liu et al. 2007; Lin et al. 2016; Wang et al. 2017), resulting in a decrease in percentage amylopectin and a subsequent increase in percentage amylose. The recessive mutant *ae/sbe2b* decreased the total activities of SBEs to approximately 71% of the WT level and increased the percentage amylose of maize kernel starch up to 70%, resulting in a high-amylose maize (Campbell et al. 2007; Jiang et al. 2010; Liu et al. 2015). All the 84 bases of the ninth exon of the *SBEIIb* gene in GEMS-0067 were completely deleted (Fig. 1b), thereby resulting in the percentage amylose of GEMS-0067 increasing to 72.95% (Table 1), a value similar to that of the high-amylose line (He et al. 2020); these results suggested that this germplasm line was derived from the same source as the high-amylose line. Thus, the increased amylose concentration of the maize germplasm might have been due to the mutation in the *SBEIIb* gene.

Another important topic to be mentioned is the relationship between defective SBEIIb activity and the morphology of starch granules in the mature endosperm. The dose-effect of SBE is the main cause of the production of heteromorphous starch granules in endosperm. The starches subjected to defective SBEIIb activity from weak to strong during starch development gradually increase the number of long branched chains of amylopectin and decrease the degree of branching of amylopectin, thus resulting in formation of heteromorphous starch granules (Wellner et al. 2011; Liu et al. 2013; Chen et al. 2017). SBEIIb contains four heterogeneous starches: polygonal, aggregate, elongated and hollow starch (Wang et al. 2018a). These traits apparently arise from inhibition of SBE activity. The characteristic features of high-amylose maize starch were observed under optical microscopy and scanning electron microscopy (Figs. 2 , 6b–d;). The kernels of GEMS-0067 were a little more shrunken, wrinkled, and duller than those of WT (Fig. 6a, b). The individual or aggregated, elongated granules with irregular depressions and small sub-granules (Fig. 2), as well as the darker staining of the endosperm by I_2/KI solution (Fig. 6c, d), are phenotypes typical of the recessive mutant *ae/sbe2b*, findings which are consistent with previous reports (Li et al. 2008; Wellner et al. 2011; Jiang et al. 2013; Cai et al. 2014; Wang et al. 2018b). Moreover, because of the differences in physicochemical properties between amylose and amylopectin, the results of amylose concentration determination were fully consistent with the iodine staining results: the higher the amylose concentration, the darker the staining. Thus,

iodine staining of the endosperm serves as an appropriate rapid, inexpensive, and non-destructive screening tool to detect starch composition. The advantages of I_2/KI solution staining are that it allows for observation of the starch granules in endosperm cells in situ, and that, because the granules are sectioned, variations in staining intensity and color (i.e., amylose concentration) within granules can be discerned according to the color differences.

The *SBEIIb* gene mutation also significantly affects the physicochemical properties of starch (Bear et al. 1958). Therefore, further research is required to study the correlation between amylose concentration and the pasting properties, thermal properties and chain length distribution. Starch pasting properties are influenced by a variety of factors including amylose concentration, granular morphology, architecture and integrity, amylopectin structure and the composition of non-starch components (Vamadevan and Bertoft 2015). Breakdown viscosity has been reported to decrease in starch with increasing amylose concentration (Case et al. 1998). Shorter chain lengths tend to destabilize the ordered arrangements of double helices in starch granules, thereby decreasing the thermal stability, whereas the interactions of starch molecules in the granules are reinforced by an increase in amylose concentration, thus increasing the thermal stability (Vamadevan and Bertoft 2015).

The gelatinization temperature of GEMS-0067 starch was recorded as > 95 °C because it was higher than the upper limit of the heating temperature of the differential scanning calorimeter. The viscosity of starch was increased, along with its gelatinization, during gradual heating due to the absorption of water and loss of starch structure (Ji et al. 2004; Singh et al. 2010). Moreover, with the influence of *SBEIIb*-defective lines, the number of long chains increased whereas the branching degree of amylopectin decreased, resulting in the change of amylose concentration and amylopectin chain length distribution, which could further affect the pasting properties of the starch. In other words, the higher gelatinization temperature of GEMS-0067 starch was also related to the greater chain length (Singh et al. 2010). With reference to Hanashiro et al. (1996), in GEMS-0067 starch, the percentage of short chains was lower, whereas the percentages of medium chains and long chains were higher (Fig. 5). The significantly lower peak viscosity, through viscosity, breakdown viscosity, final viscosity, setback viscosity, and gelatinization enthalpy (Fig. 3; Tables 2 and 3), and significantly higher peak time, gelatinization temperature, and transition temperatures (T_o, T_p, and T_c; Tables 2 and 3), as well as the inconspicuous absorption peak (Fig. 4) of GEMS-0067 starch, implied that gelatinization initiation of GEMS-0067 starch needed much more energy to heat than the WT starch, because of the former's high proportion of amylose (Table 1), high percentage of medium and long chains, and closer and more orderly arrangement of starch granules (Fig. 5). Moreover, because the *SBEIIb* gene mutation eliminated a major form of SBE in the endosperm, and because of the unique physicochemical properties of high-amylose starch, long linear chains form double helices that pack together into crystallites during gelatinization and cooling. These structures are resistant to attack by α-amylases in the upper gut. Thus, starches with high amylose concentration are generally more resistant to digestion (Man et al. 2012; Tuncel et al. 2019).

Increased amylose concentrations also affect yield. Negative correlations between percentage amylose and starch concentration, as well as kernel-filling characteristics, have been reported in most of the high-amylose germplasm lines, with high-amylose concentration traits exhibiting side effects, and causing a significant reduction in total yield, which was essentially impossible to avoid by conventional breeding (Zhao et al. 2015). In some high-amylose lines with recessive mutations of some other modifier genes (such as *sbe1*), the kernel-filling characteristics were less affected, but the amylose proportion was not as high as in the *ae/sbe2b* mutant lines (Zhang et al. 2020). Kernel mass and kernel number were also determined in the current study as measures of maize yield, the most important agronomic trait. In the present study, the shrinkage of GEMS-0067 kernels resulted in the significant decrease in its 100-kernel mass (Fig. 6; Table 4). However, the significant increase in the number of kernels per row in GEMS-0067 (28, versus 26 for WT) offset some of this loss. The kernel mass per ear of GEMS-0067 was only 8.3% lower than its WT (Table 4). A previous study had also confirmed the possibility of creating high-amylose hybrid lines without a serious reduction in total starch (Bear et al. 1958). In our study, the amylose proportion of GEMS-0067 on a dry mass basis was 72.95%, a value 178% higher than that of the WT

(26.26%), whereas the single grain mass of GEMS-0067 was 0.25 g, a value 20% less than that of the WT (0.3 g). In the presence of the *SBEIIb* gene mutation, the grain yield decreased 17%, whereas the amylose proportion per grain biomass increased 131%; the ratio of these two indexes was 0.1298 (Table 4). Although the high-amylose concentration was negatively correlated with yield, the effect of *SBEIIb* gene mutation on increasing the amylose concentration far exceeded the side effect of decreasing the yield, particularly given the considerable value of amylose in the starch industry and nutraceutical fields, thereby determining the value of GEMS0067 in breeding.

In summary, the *ae/sbe2b* mutant is defective in the starch-branching enzyme SBEIIb, which plays an important role in maize endosperm starch synthesis. The mutations in this gene present in GEMS-0067 caused a significant increase in the amylose proportion of maize starch and also affected other traits. The present study demonstrated that the phenotypic characteristics and physicochemical properties affected, including agronomic traits, kernel morphology and glossiness, starch concentration, percentage amylose, pasting properties, thermal properties, and chain length distribution, could be largely correlated with the differences in the structure caused by the *ae* gene mutation. These results are in accordance with our original hypothesis. These experimental results provide information that may guide future studies on the physicochemical properties of high-amylose starch and aid in elucidating the function of the *ae* gene for the utilization of high-amylose starch and maize breeding. To better understand how the mutant gene affects starch synthesis, and whether enzymes encoded by the gene play important roles in the starch biosynthetic process and starch physicochemical properties, further research by our team is in progress to knock out the *SBEIIb* gene by CRISPR/Cas9, using GEMS-0067 as the reference material, to create additional maize germplasm with even higher percentage amylose. This future work will focus on the similarities and differences between the gene-edited maize and the GEMS-0067 line (with the *ae* genetic mutation) in terms of molecular, phenotypic, and physicochemical characteristics. It will be helpful for researchers to analyze the target genotypes, to facilitate the design of gene-modified plants producing high-amylose starches, and to further understand the mechanisms through which the mutant genes affect starch synthesis and physicochemical properties, in order to achieve practical applications.

Acknowledgements This research was funded by the Programs of Science and Technology Department of Sichuan (Grant Nos. 2018JY0470 and 2020YJ0353) and the National Natural Science Foundation of China (Grant No. 32001552). We thank International Science Editing (http://www.internationalscienceediting.com) for editing this manuscript.

Author contributions Conceptualization, CX and FF; methodology, NH; software, NH; investigation, NH; resources, CX; data curation, WL; writing—original draft preparation, NH; writing—review and editing, WL; supervision, CX; funding acquisition, WL. All authors have read and agreed the published version of the manuscript.

Declarations

Conflict of interest The authors declare that they have no conflict of interest.

References

Andorf C, Beavis WD, Hufford M, Smith S, Suza WP, Wang K, Woodhouse M, Yu J, Lübberstedt T (2019) Technological advances in maize breeding: past, present and future. Theor Appl Genet 132:817–849. https://doi.org/10.1007/s00122-019-03306-3

Bear R, Vineyard M, MacMasters M, Deatherage W (1958) Development of "Amylomaize"—corn hybrids with high amylose starch: II. Results of breeding efforts 1. Agron J. https://doi.org/10.2134/agronj1958.00021962005000100010x

Cai C, Lin L, Man J, Zhao L, Wang Z, Wei C (2014) Different structural properties of high-amylose maize starch fractions varying in granule size. J Agric Food Chem 62:11711–11721. https://doi.org/10.1021/jf503865e

Campbell MR, Jane J, Pollak L, Blanco M, O'Brien A (2007) Registration of maize germplasm line GEMS-0067. J Plant Regist 1:60–61. https://doi.org/10.3198/jpr2006.10.0640crg

Case SE, Capitani T, Whaley JK, Shi YC, Trzasko P, Jeffcoat R, Goldfarb HB (1998) Physical properties and gelation behavior of a low-amylopectin maize starch and other high-amylose maize starches. J Cereal Sci 27:301–314. https://doi.org/10.1006/jcrs.1997.0164

Chen X, Du X, Chen P, Guo L, Xu Y, Zhou X (2017) Morphologies and gelatinization behaviours of high-amylose maize starches during heat treatment. Carbohydr Polym 157:637–642. https://doi.org/10.1016/j.carbpol.2016.10.024

Fuwa H, Inouchi N, Glover DV, Fujita S, Sugihara M, Yoshioka S, Yamada K, Sugimoto Y (1999) Structural and physicochemical properties of endosperm starches possessing different alleles at the *amylose-extender* and *waxy* locus in maize (*Zea mays* L.). Starch-Stärke 51:147–151

Gibson TS, Solah VA, McCleary BV (1997) A procedure to measure amylose in cereal starches and flours with concanavalin A. J Cereal Sci 25:111–119. https://doi.org/10.1006/jcrs.1996.0086

Glaring MA, Koch CB, Blennow A (2006) Genotype-specific spatial distribution of starch molecules in the starch granule: a combined CLSM and SEM approach. Biomacromolecules 7:2310–2320. https://doi.org/10.1021/bm060216e

Goren A, Ashlock D, Tetlow IJ (2018) Starch formation inside plastids of higher plants. Protoplasma 255:1855–1876. https://doi.org/10.1007/s00709-018-1259-4

Guan HP, Preiss J (1993) Differentiation of properties of maize branching isozymes. Plant Physiol 102:1269–1273

Hanashiro I, Abe J, Hizukuri S (1996) A periodic distribution of the chain length of amylopectin as revealed by high-performance anion-exchange chromatography. Carbohydr Res 283:151–159. https://doi.org/10.1016/0008-6215(95)00408-4

He W, Liu X, Lin L, Xu A, Hao D, Wei C (2020) The defective effect of starch branching enzyme IIb from weak to strong induces the formation of biphasic starch granules in amylose-extender maize endosperm. Plant Mol Biol 103:355–371. https://doi.org/10.1007/s11103-020-00998-w

Hunt HV, Moots HM, Graybosch RA, Jones H, Parker M, Romanova O, Jones MK, Howe CJ, Trafford K (2013) Waxy phenotype evolution in the allotetraploid cereal broomcorn millet: mutations at the *GBSSI* locus in their functional and phylogenetic context. Mol Biol Evol 30:109–122. https://doi.org/10.1093/molbev/mss209

Jeon J-S, Ryoo N, Hahn T-R, Walia H, Nakamura Y (2010) Starch biosynthesis in cereal endosperm. Plant Physiol Biochem 48:383–392. https://doi.org/10.1016/j.plaphy.2010.03.006

Ji Y, Pollak LM, Duvick S, Seetharaman K, Dixon PM, White PJ (2004) Gelatinization properties of starches from three successive generations of six exotic corn lines grown in two locations. Cereal Chem 81:59–64. https://doi.org/10.1094/CCHEM.2004.81.1.59

Jiang H, Srichuwong S, Campbell M, Jane J (2010) Characterization of maize *amylose-extender* (*ae*) mutant starches. Part III: structures and properties of the Naegeli dextrins. Carbohydr Polym 81:885–891. https://doi.org/10.1016/j.carbpol.2010.03.064

Jiang L, Yu X, Qi X, Yu Q, Deng S, Bai B, Li N, Zhang A, Zhu C, Liu B, Pang J (2013) Multigene engineering of starch biosynthesis in maize endosperm increases the total starch content and the proportion of amylose. Transgenic Res 22:1133–1142. https://doi.org/10.1007/s11248-013-9717-4

Kim K-N, Fisher D, Gao M, Guiltinan M (1998) Molecular cloning and characterization of the *amylose-extender* gene encoding starch branching enzyme IIB in maize. Plant Mol Biol 38:945–956. https://doi.org/10.1023/A:1006057609995

Koch K, Gillgren T, Stading M, Andersson R (2010) Mechanical and structural properties of solution-cast high-amylose maize starch films. Int J Biol Macromol 46:13–19. https://doi.org/10.1016/j.ijbiomac.2009.10.002

Li L, Jiang H, Campbell M, Blanco M, Jane J (2008) Characterization of maize *amylose-extender* (*ae*) mutant starches. Part I: relationship between resistant starch contents and molecular structures. Carbohydr Polym 74:396–404. https://doi.org/10.1016/j.carbpol.2008.03.012

Li C, Huang Y, Huang R, Wu Y, Wang W (2018) The genetic architecture of amylose biosynthesis in maize kernel. Plant Biotechnol J 16:688–695. https://doi.org/10.1111/pbi.12821

Lin L, Guo D, Huang J, Zhang X, Zhang L, Wei C (2016) Molecular structure and enzymatic hydrolysis properties of starches from high-amylose maize inbred lines and their hybrids. Food Hydrocoll 58:246–254. https://doi.org/10.1016/j.foodhyd.2016.03.001

Liu J, Rong T, Li W (2007) Mutation loci and intragenic selection marker of the granule-bound starch synthase gene in waxy maize. Mol Breed 20:93–102. https://doi.org/10.1007/s11032-006-9074-6

Liu D, Parker ML, Wellner N, Kirby AR, Cross K, Morris VJ, Cheng F (2013) Structural variability between starch granules in wild type and in *ae* high-amylose mutant maize kernels. Carbohydr Polym 97:458–468. https://doi.org/10.1016/j.carbpol.2013.05.013

Liu D, Wellner N, Parker ML, Morris VJ, Cheng F (2015) In situ mapping of the effect of additional mutations on starch granule structure in *amylose-extender* (*ae*) maize kernels. Carbohydr Polym 118:199–208. https://doi.org/10.1016/j.carbpol.2014.11.006

Man J, Yang Y, Zhang C, Zhou X, Dong Y, Zhang F, Liu Q, Wei C (2012) Structural changes of high-amylose rice starch residues following in vitro and in vivo digestion. J Agric Food Chem 60:9332–9341. https://doi.org/10.1021/jf302966f

Maroof S, Soliman KM, Jorgensen RA, Allard RW (1985) Ribosomal DNA spacer-length polymorphisms in barley: mendelian inheritance, chromosomal location, and population dynamics. Proc Natl Acad Sci USA 81:8014–8018. https://doi.org/10.1073/pnas.81.24.8014

Myers AM, Morell MK, James MG, Ball SG (2000) Recent progress toward understanding biosynthesis of the amylopectin crystal. Plant Physiol 122:989–997. https://doi.org/10.1104/pp.122.4.989

Raigond P, Ezekiel R, Raigond B (2015) Resistant starch in food: a review. J Sci Food Agric 95:1968–1978. https://doi.org/10.1002/jsfa.6966

Singh S, Singh N, Isono N, Noda T (2010) Relationship of granule size distribution and amylopectin structure with pasting, thermal, and retrogradation properties in wheat starch. J Agric Food Chem 58:1180–1188. https://doi.org/10.1021/jf902753f

Song Y, Li X, Zhong Y (2019) Optimization of butter, xylitol, and high-amylose maize flour on developing a low-sugar cookie. Food Sci Nutr 7:3414–3424. https://doi.org/10.1002/fsn3.1160

Tuncel A, Corbin KR, Ahn-Jarvis J, Harris S, Hawkins E, Smedley MA, Harwood W, Warren FJ, Patron NJ, Smith AM (2019) Cas9-mediated mutagenesis of potato starch-branching enzymes generates a range of tuber starch phenotypes. Plant Biotechnol J 17:2259–2271. https://doi.org/10.1111/pbi.13137

Vamadevan V, Bertoft E (2015) Structure-function relationships of starch components. Starch-Stärke 67:55–68. https://doi.org/10.1002/star.201400188

Wang J, Hu P, Chen Z, Liu Q, Wei C (2017) Progress in high-amylose cereal crops through inactivation of starch branching enzymes. Front Plant Sci 8:469. https://doi.org/10.3389/fpls.2017.00469

Wang J, Hu P, Lin L, Chen Z, Liu Q, Wei C (2018a) Gradually decreasing starch branching enzyme expression is responsible for the formation of heterogeneous starch granules. Plant Physiol 176:582–595. https://doi.org/10.1104/pp.17.01013

Wang W, Guan L, Seib PA, Shi YC (2018b) Settling volume and morphology changes in cross-linked and unmodified starches from wheat, waxy wheat, and waxy maize in relation to their pasting properties. Carbohydr Polym 196:18–26. https://doi.org/10.1016/j.carbpol.2018.05.009

Wei C, Qin F, Zhou W, Xu B, Chen C, Chen Y, Wang Y, Gu M, Liu Q (2011) Comparison of the crystalline properties and structural changes of starches from high-amylose transgenic rice and its wild type during heating. Food Chem 128:645–652. https://doi.org/10.1016/j.foodchem.2011.03.080

Wellner N, Georget DMR, Parker ML, Morris VJ (2011) In situ Raman microscopy of starch granule structures in wild type and *ae* mutant maize kernels. Starch-Stärke 63:128–138. https://doi.org/10.1002/star.201000107

Yang XS, Wang LL, Zhou XR, Shuang SM, Zhu ZH, Li N, Li Y, Liu F, Liu SC, Lu P, Ren GX, Dong C (2013) Determination of protein, fat, starch, and amino acids in foxtail millet [*Setaria italica* (L.) Beauv.] by fourier transform near-infrared reflectance spectroscopy. Food Sci Biotechnol 22:1595–1500. https://doi.org/10.1007/s10068-013-0243-1

Zhang X, Chen Y, Zhang R, Zhong Y, Luo Y, Xu S, Liu J, Xue J, Guo D (2016) Effects of extrusion treatment on physicochemical properties and in vitro digestion of pregelatinized high amylose maize flour. J Cereal Sci 68:108–115. https://doi.org/10.1016/j.jcs.2016.01.005

Zhang X, Gao X, Li Z, Xu L, Li Y, Zhang R, Xue J, Guo D (2020) The effect of amylose on kernel phenotypic characteristics, starch-related gene expression and amylose inheritance in naturally mutated high-amylose maize. J Integr Agric 19:1554–1564. https://doi.org/10.1016/S2095-3119(19)62779-6

Zhao Y, Li N, Li B, Li Z, Xie G, Zhang J (2015) Reduced expression of starch branching enzyme IIa and IIb in maize endosperm by RNAi constructs greatly increases the amylose content in kernel with nearly normal morphology. Planta 241:449–461. https://doi.org/10.1007/s00425-014-2192-1

Zhong Y, Liu L, Qu J, Li S, Blennow A, Seytahmetovna S, Liu X, Guo D (2020) The relationship between the expression pattern of starch biosynthesis enzymes and molecular structure of high amylose maize starch. Carbohydr Polym 247:116681. https://doi.org/10.1016/j.carbpol.2020.116681